TISSUE ENGINEERING: Part A
Volume 23, Numbers 5 and 6, 2017

DOI: 10.1089/ten.tea.2016.0246

termis
Tissue Engineering
& Regenerative Medicine
International Society

ORIGINAL ARTICLE

A New Vertebral Body Replacement Strategy Using Expandable Polymeric Cages

Xifeng Liu, PhD,[1,2] Alex Paulsen, BS,[2] Hugo Giambini, PhD,[2] Ji Guo, MD,[2] A. Lee Miller II, PhD,[2] Po-Chun Lin, MD,[2] Michael J. Yaszemski, MD, PhD,[1,2] and Lichun Lu, PhD[1,2]

We have developed a novel polymeric expandable cage that can be delivered via a posterior-only surgical approach for the treatment of noncontained vertebral defects. This approach is less invasive than an anterior-only or combined approach and much more cost-effective than currently used expandable metal cages. The polymeric expandable cage is composed of oligo poly(ethylene glycol) fumarate (OPF), a hydrogel that has been previously shown to have excellent nerve and bone tissue biocompatibility. OPF hydrogel cages can expand to twice their original diameter and length within a surgical time frame following hydration. Modulation of parameters such as polymeric network crosslink density or the introduction of charge to the network allowed for precise expansion kinetics. To meet specific requirements due to size variations in patient vertebral bodies, we fabricated a series of molds with varied diameters and explored the expansion kinetics of the OPF cages. Results showed a stable expansion ratio of approximately twofold to the original size within 20 min, regardless of the absolute value of the cage size. Following implantation of a dried OPF cage into a noncontained vertebral defect and its *in situ* expansion with normal saline, other augmentation biomaterials, such as poly(propylene fumarate) (PPF), can be injected to the lumen of the OPF cage and allowed to crosslink *in situ*. The OPF/PPF composite scaffold can provide the necessary rigidity and stability to the augmented spine.

Keywords: tissue engineering, spine, vertebral body reconstruction, biomaterials, hydrogel

Introduction

Multiple pathologies can affect vertebral bodies, including tumor, fractures, and infection, reducing spinal stability and increasing risk for further vertebral or nervous tissue injury.[1] The spinal column is the most common site of bone metastasis and occurs in one-third of cancers.[2–5] Vertebral body injury has historically been treated with corpectomy of the affected body and adjacent intervertebral discs. This defect can then be replaced with autografts, allografts, or a variety of fixed and expandable titanium or polymeric cages[6] with the purpose of reducing pain, decompression of neural elements, spinal stabilization, and resection of the malignancy.[7]

Bone grafts used to reconstruct the anterior column have been associated with complications such as pseudoarthrosis, graft collapse, kyphotic deformity, and graft extrusion.[8,9] Titanium cages have proven to be an effective method of treatment, providing instantaneous stability, correction of kyphotic deformity, and relief of cord compression. However, these implants sometimes require both an anterior and a posterior surgical exposure. On the contrary, the use of expandable titanium cages has enabled an alternative posterior-only surgical approach to the more invasive anterior-only or combined approach.[10] Yet, in addition to its high costs, titanium instrumentation does not allow for natural healing in those patients for whom a biologic reconstruction is desired. In addition, the modulus is much higher compared to natural bone, which may lead to injury of adjacent vertebral bodies. These open surgical procedures become difficult to bear by these delicate patients, posing a greater surgical risk and a challenging recovery.[11] With a demographic shift toward an elderly population, there exists a need for a less invasive surgical approach for the repair of vertebral body defects so commonly present in this population.[12]

Biocompatible and biodegradable polymers, such as poly(L-lactic acid) (PLLA),[13] poly(ε-caprolactone),[14–16] poly(propylene fumarate) (PPF),[17,18] poly(ethylene glycol) (PEG),[19] and oligo poly(ethylene glycol) fumarate (OPF),[20] have been used for various tissue engineering applications showing excellent *in vitro* and *in vivo* results. For example, PLLA polymer was reported to have desirable biocompatibility and biodegradability

Departments of [1]Physiology and Biomedical Engineering and [2]Orthopedic Surgery, Mayo Clinic, Rochester, Minnesota.

in *in vitro* studies, and attractive tissue affinities without inflammation in *in vivo* studies.[21,22] With inherent crosslinkable fumarate bonds, PPF polymer can be photocrosslinked or chemical-crosslinked to form a biocompatible network.[23] A number of copolymers/blends developed on the basis of crosslinkable PPF were explored for bone tissue engineering applications.[17,24–26] Good biocompatibility and cellular behavior were reported in *in vitro* studies and encouraging results were demonstrated supporting bone regeneration in animal work.[27–30]

PEG is a biocompatible hydrophilic polymer that has been studied for many years in the bone tissue engineering field.[22,31] As a derivative of PEG, the OPF polymer has been synthesized by esterification of PEG with fumaric acid.[32] The double bonds in the fumaric acid segments provide a crosslinking ability to the OPF chains, whereas the PEG segments allow a high degree of swelling when exposed to an aqueous environment. The hydrated OPF gel is biocompatible and biodegradable through hydrolysis of inherent ester bonds.[33,34] The water content, crosslinking density, and modulus of crosslinked OPF hydrogel can be further modulated based on specific purposes and goals.[35]

To overcome the current spine surgery limitations using metal cages, in this study, we developed a novel biodegradable polymeric containment device to replace the missing structural portion of a vertebral body that has a noncontained metastatic defect. The OPF cages were fabricated by photocrosslinking OPF blend in a mold. As described in Figure 1a, on rehydration, these cages were able to expand in size to a predetermined diameter and length. This degree of expansion would enable a less invasive posterior-only surgical approach for insertion of the scaffold (Fig. 1b). Once expanded *in vivo*, the implant would be filled with PPF to provide structural support and rigidity to the spine, allow for bone regeneration, and sustained release of chemotherapeutic and/or antibiotic agents (Fig. 1b).

Materials and Methods

The expansion kinetics of OPF cages were explored by altering the molecular weight, charge, and scaffold mold diameter. The effects of these changes were quantified by observing the expansion rates of scaffold length, diameter, and mass under physiologic conditions.

Materials

PEG, fumaryl chloride, potassium carbonate (K_2CO_3), benzoyl peroxide (BPO), N,N-dimethyl-o-toluidine (DMT), and 1-vinyl-2-pyrrolidinone (NVP) were purchased from Sigma Aldrich Co. (Milwaukee, WI). Methylene chloride (CH_2Cl_2) and other common solvents were purchased from Fisher (Pittsburgh, PA) and used as received. All other reagents/chemicals were purchased from Fisher or Sigma unless noted otherwise.

Synthesis of OPF

OPF2k and OPF10k were synthesized using fumaryl chloride and PEG with number-average molecular weight (Mn) of 2000 and 10,000, respectively, according to previous reports.[36–38] Briefly, PEG (50 g) with designated molecular weight was azeotropically distilled in toluene and dissolved in anhydrous CH_2Cl_2 (500 mL) in a three-neck flask. The PEG/CH_2Cl_2 reaction system was placed in an ice bath and purged with nitrogen for 10 min. K_2CO_3 powder (20 g) was first added, with a subsequent dropwise addition of fumaryl chloride (1:1 in molar ratio to PEG) under stirring conditions. The reaction was kept at room temperature for 48 h and then centrifuged to remove the solid K_2CO_3 powder. The filtrate was concentrated by rotary evaporation, precipitated in cold diethyl ether, fully dried in vacuum, and stored at −20°C for future use.

Fabrication of scaffolds with variable molecular weight

The synthesized OPF of molecular weights 2000 and 10,000 Da was used to fabricate scaffolds of 10 mm diameter. One gram of OPF2k, 0.05 g BAPO, 0.1 g NVP, and 2 mL CH_2Cl_2 were combined into a flask. The mixture was vortexed until all solutes were dissolved. After greasing the metal rod of the mold, 3 mL of the resin was added to the scaffold mold. This was placed in a UV oven to initiate crosslinking. After 60 min, the center metal rod of the mold was removed and the scaffold was placed back in the UV oven for an additional 2 h. The scaffold was placed in the hood at room temperature overnight to fully dry. OPF10k was fabricated following the same steps, however, the amount of the ingredients was altered as follows: 1 g OPF10k, 0.15 g BAPO, 0.3 g NVP, and 2 mL CH_2Cl_2.

Fabrication of scaffolds with variable charge

The effect of negative charge on swelling time of these scaffolds was studied by both chemically crosslinking sodium methacrylate (SMA) within the polymer network or physically infiltrating SMA into the network. For the chemical crosslinking method, the OPF monomer was dissolved in CH_2Cl_2, added to varied concentrations of SMA (0%, 5%, 10%, and 20%, w/w to OPF), and then crosslinked under UV irradiation. For the physical incorporation method, the crosslinked OPF scaffold was soaked for 1 day in ddH_2O containing varied concentrations of SMA (0%, 0.5%, 2.5%, and 10%). Scaffolds were subsequently dried overnight in a 70°C oven.

Fabrication of scaffolds with variable diameter

OPF2k resin was fabricated as described above; however, the diameter of the scaffold mold was increased from 10 to 15 mm. Both scaffolds were soaked in 2.5% SMA to achieve a final concentration of 12% SMA.

Expansion kinetics

Expansion rate was evaluated on scaffolds with variable molecular weight, charge, and diameter by immersing each 10 mm section in 50 mL of phosphate-buffered saline (PBS) solution at 37°C. The mass, length, and diameter were measured at serial time points from 0 to 80 min. Digital pictures of each measurement were taken at each time point. The inside volume of each scaffold was calculated using the respective diameter and length.

Mechanical testing

Mechanical properties of crosslinked OPF scaffolds of 10 and 15 mm diameter were determined using a dynamic

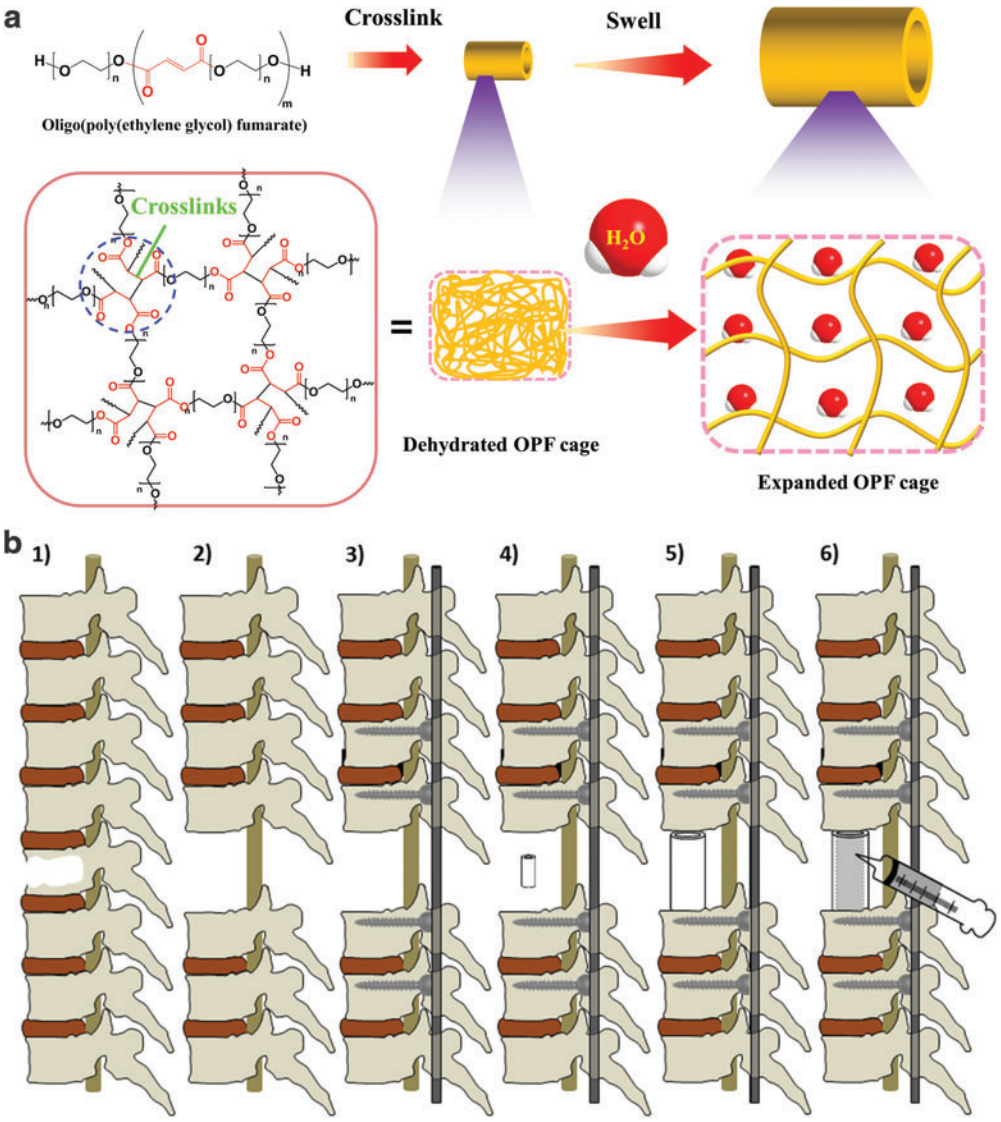

FIG. 1. **(a)**. Crosslinked OPF cages have the ability to expand in size when placed in aqueous solution. **(b)** Schematic demonstration of the insertion of dried OPF cage. 1: Spine with single vertebral metastasis; 2: removal of affected vertebral body and adjacent intervertebral discs; 3: posterior instrumentation; 4: insertion of dried OPF hollow graft; 5: graft *in situ* expansion to predetermined size; 6: injection of crosslinkable supportive PPF into cage lumen and *in situ* crosslinking. OPF, oligo poly(ethylene glycol) fumarate; PPF, poly(propylene fumarate). Color images available online at www.liebertpub.com/tea

mechanical analyzer (RSA-G2, TA instruments). Compressive stress–strain curves for OPF cages before and after swelling were obtained at a constant linear rate of 0.01 mm/s. Compressive moduli were calculated from the slope of the linear region in the stress–strain curves and averaged with two samples.

In situ *swelling and injection*

OPF cages were placed in a metal mold with two iron rods mimicking the *in vivo* vertebral body defect conditions. After the cages were fully swelled, a formulation of crosslinkable PPF with initiators and accelerators was prepared and injected, according to previous reports.[18,38] Briefly, 3.0 g of PPF was dissolved in 1.0 mL CH_2Cl_2 and mixed thoroughly. One hundred microliters of initiator (0.2 g BPO dissolved in 1 mL NVP) was added and mixed with the polymer solution. Eighty microliters of accelerator (20 μL of DMT dissolved in 980 μL CH_2Cl_2) was quickly added and the PPF/BPO/NVP/DMT formulation was then transferred into a syringe and carefully injected into the swelled OPF scaffolds. The biomaterial system was kept at room temperature overnight to allow for *in situ* polymerization and a crosslinked polymer network inside the expandable scaffolds.

Results

Effect of crosslink density on swelling

The expansion and swelling over time of the 10-mm-diameter cages fabricated with OPF with molecular weight of 2k and 10k were studied. As shown in Figure 2a and b, there is a significant visual radial and longitudinal expansion over a 120-min immersion period for both types of cages. However, visually, the 2k OPF construct (Fig. 2a) presented a more homogeneous geometrical structure compared to the

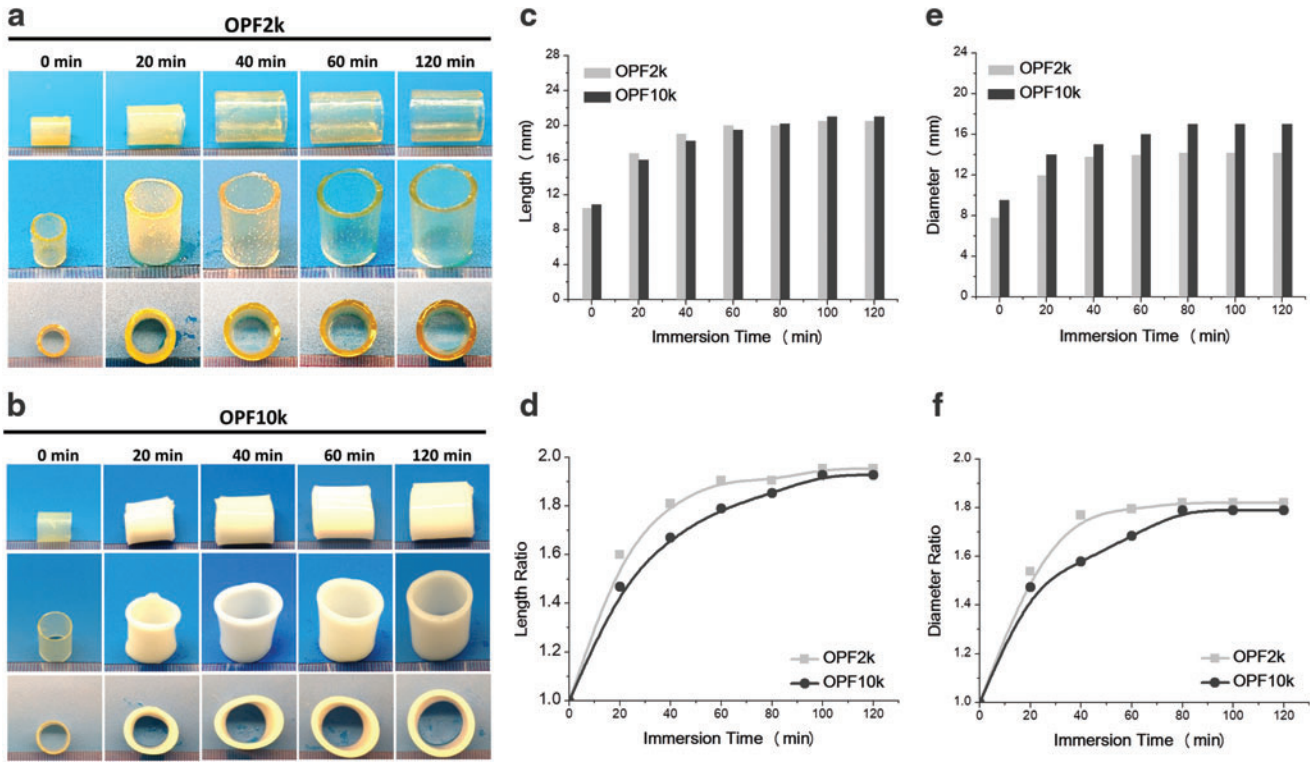

FIG. 2. Photographs of shape evaluation of expandable cages fabricated with varied molecular weight **(a)** OPF2k and **(b)** OPF10k. **(c)** Absolute length and **(d)** relative ratio normalized to the original length were calculated over an immersion time to 120 min in PBS. **(e)** Absolute diameter and **(f)** ratio change of cages fabricated by both OPF2k and OPF10k polymers were also investigated. PBS, phosphate-buffered saline. Color images available online at www.liebertpub.com/tea

10k OPF scaffold (Fig. 2b). Moreover, differences in expansion kinetics are clearly observed at the 40- and 60-min time intervals.

Both OPF scaffolds showed a significant increase in their length during the first 20 min (Fig. 2c–f). The final length after 120 min was approximately 20 mm (Fig. 2c). The length of the 2k OPF molecular weight scaffold tended to plateau around 60 min, while a longer time period was required for the 10k scaffold, as shown in Figure 2d. A similar trend was observed on the expanded scaffold diameter. The OPF2k cages achieved an approximate constant diameter at the 40-min time point, while the 10k cage required double the time (Fig. 2e). Diameter ratios showed a similar trend as the length ratio change, as shown in Figure 2f.

Absolute mass and volume for both molecular weight scaffolds are shown in Figure 3. The OPF2k cage achieved an almost constant mass of 1000 mg at the 60-min immersion time (Fig. 3a). In contrast, the OPF10k cage showed a continuous increase in mass over time, until reaching a plateau of about 1600 mg around 120 min. Mass ratio increased approximately fourfold for the OPF2k scaffolds, while the OPF10k scaffolds reached a maximum mass change of around 12-fold, compared to its initial value (Fig. 3b). This phenomenon can be due to a higher water absorption capability of the OPF10k cages. A higher absolute volume was also observed for the OPF10k cage compared with that of the OPF2k cage (Fig. 3c). The maximum volume ratio of the OPF2k sample at the 60-min time point was about sixfold compared to a fivefold increase in the OPF10k cage (Fig. 3d).

Effect of charge on swelling

Since the OPF2k showed better expansion kinetics (length, diameter, mass, and volume ratios) compared to the OPF10k scaffold, this molecular weight composition was chosen to evaluate chemical crosslinking of SMA into the OPF network and physical incorporation of SMA into the crosslinked OPF network (Fig. 4a, b). As shown in Figure 4a, the chemical crosslinking process covalently and permanently linked the SMA molecules into the polymer network. Expansion kinetics showed a limited effect of this process in improving the swelling time of the OPF cage with varying SMA compositions. On the contrary, the incorporated SMA small molecules produced undesired side effects by largely restricting the final swelling ability of the OPF cage (Fig. 4c).

A schematic of charge incorporation by physical adsorption of SMA into the crosslinked network is shown (Fig. 4b). By measuring the initial mass and the mass after soaking, final concentrations of absorbed SMA in the scaffolds were 0%, 2.4%, 12%, and 48% for scaffolds soaked in 0%, 0.5%, 2.5%, and 10% solution, respectively. The results demonstrated a significant decrease in swelling time, as shown in Figure 4d. In addition, solely due to a physical absorption process and contrary to the chemically bonded SMA process, no side effects were observed on the final size of swelled OPF cages.

Effect of scaffold diameter on swelling

Expansion kinetics of 10- and 15-mm-diameter OPF2k scaffolds are shown in Figure 5. Top and side views of both

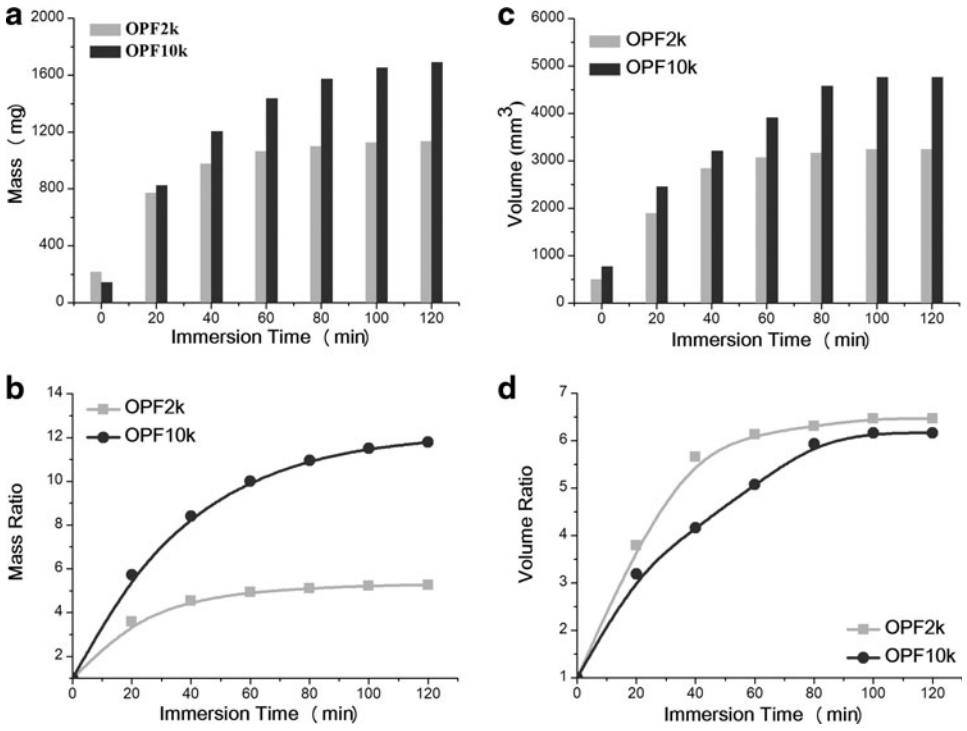

FIG. 3. **(a)** Absolute mass, **(b)** mass ratio change, **(c)** absolute volume, and **(d)** volume change of OPF2k and OPF10k scaffolds during a 120-min swelling in PBS.

cages are shown in Figure 5a and b. The absolute length, diameter, and their ratio changes with swelling time in PBS are shown in Figure 5c–f. Both cages attained a length and diameter plateau at around 30-min immersion time. The length ratio of the 10 mm cage at the 30-min time point was ~1.9, while the 15 mm cage showed a length ratio of 2 (Fig. 5d). The diameter ratio of the 10 mm cage at the 30-min time point was ~2.1, while the 15 mm cage showed a ratio value of 2 (Fig. 5f). A similar trend in the mass ratio increase was observed for both length types, with a plateau in mass around 60 min. The 10 mm cage reached a mass ratio of 7 (~1000 mg), while the 15 mm cage presented a

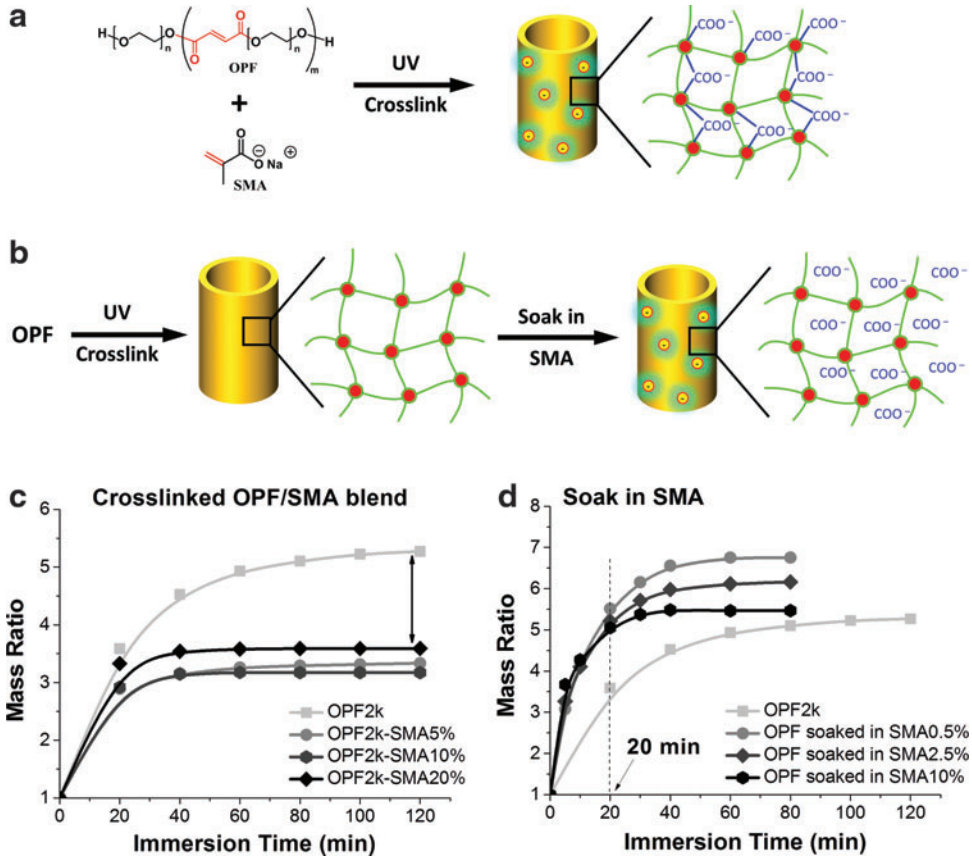

FIG. 4. Schematic of **(a)** chemically crosslinking SMA with OPF to form a polymer network with negative charges; **(b)** physical incorporation of SMA into the crosslinked OPF polymer network; **(c)** effect of chemically crosslinking SMA molecules on swelling kinetics of OPF2k scaffolds; **(d)** effect of adsorbed SMA molecules on swelling kinetics of the OPF2k scaffolds. SMA, sodium methacrylate. Color images available online at www.liebertpub.com/tea

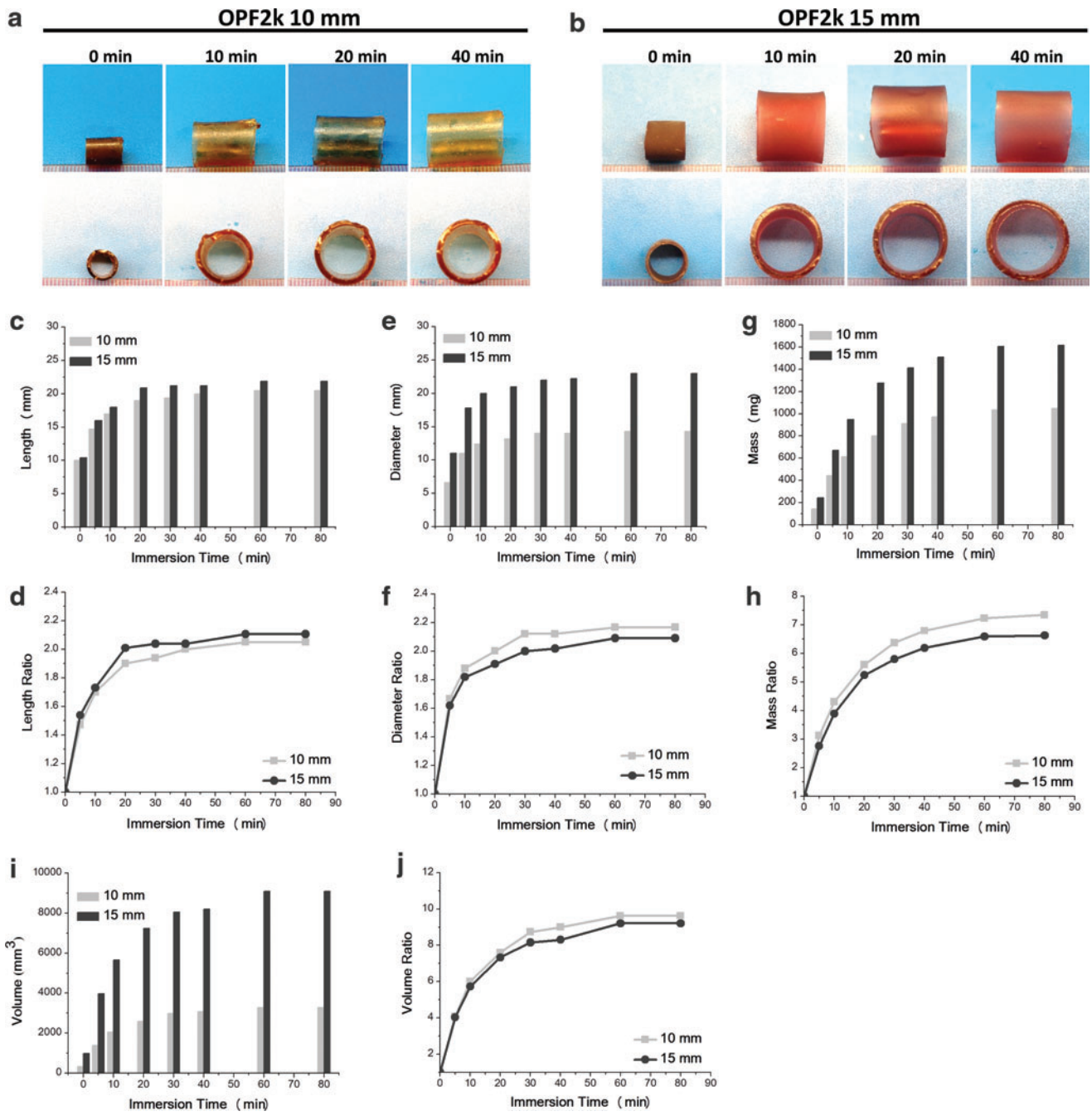

FIG. 5. Digital photographs showing the swelling process of the cages in PBS over time and their expansion kinetics. Cages were fabricated with OPF2k with **(a)** 10-mm and **(b)** 15-mm-diameter mold; **(c)** absolute length, **(d)** length ratio, **(e)** absolute diameter, **(f)** diameter ratio, **(g)** absolute mass, **(h)** mass ratio, **(i)** absolute volume, and **(j)** volume ratio. Color images available online at www.liebertpub.com/tea

ratio of 6.5 (~1600 mg), as noted in Figure 5g and h. Although a significant visual difference was observed in the absolute volume change of these two cage types (Fig. 5i), reaching a plateau at about 60 min, their ratio change was similar at about nine-fold the original size (Fig. 5j).

Mechanical properties before and after swelling

Stress versus strain curves of all four sample types (Fig. 6a, b) obtained from the mechanical compression tests are shown in Figure 6c and d. Both 10- and 15-mm-diameter dry cages presented a much steeper increase in the stress response to the applied strain when compared to their swelled counterparts (Fig. 6c). An enlarged view below 6 kPa shows a steeper increase of the 10-mm-diameter cages, in both dry and swelled conditions, than the respective 15-mm cages (Fig. 6c). Compressive moduli are shown in Figure 6d. For both 10- and 15-mm-diameter cages, the dry samples presented a larger modulus, ranging in the 328.0 ± 108.9 and 142.5 ± 19.1 kPa, respectively. On the contrary, after swelling, there was an evident decrease in the moduli of both cages (16.5 ± 6.4 kPa and 13.5 ± 7.8 kPa, respectively).

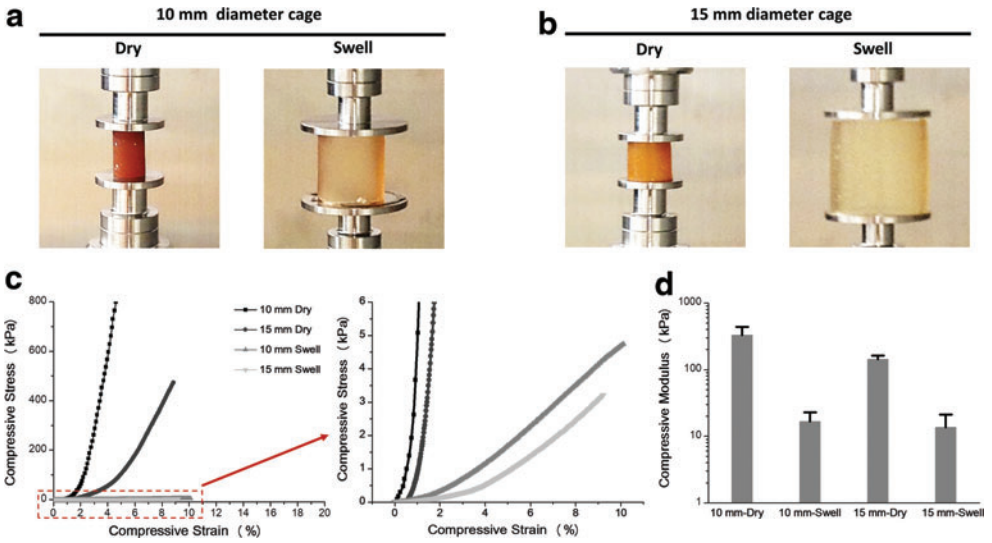

FIG. 6. Compressive testing of **(a)** 10-mm and **(b)** 15-mm-diameter OPF cages in dry and swollen states. **(c)** Stress–strain curves and enlarged region below 6 kPa. **(d)** Compressive moduli obtained from the linear region of the stress–strain curves. Color images available online at www.liebertpub.com/tea

In situ *injection and polymerization of supportive polymers*

To mimic the potential *in vivo* application, a simplified *in vitro* study was conducted. A metal mold with two metal rods mimicking vertebral bodies was manufactured, as described in Figure 7a. A gap distance was set to create an artificial defect condition and the mold was immersed in PBS with a red dye to allow for better visualization of the scaffold. Expandable crosslinked OPF cages were then inserted into the artificial defect section and observed for *in situ* swelling. The cages were able to swell to the predetermined size in ~15 min (Fig. 7b). After reaching a predetermined final swelled size, the cage then squeezes tightly between the two rods, forming a nearly closed hollow space available for injection of supportive materials. The chemical crosslinkable PPF/BPO/NVP/DMT formulation was injected using a syringe into the hollow space successfully (Fig. 7c). After injection,

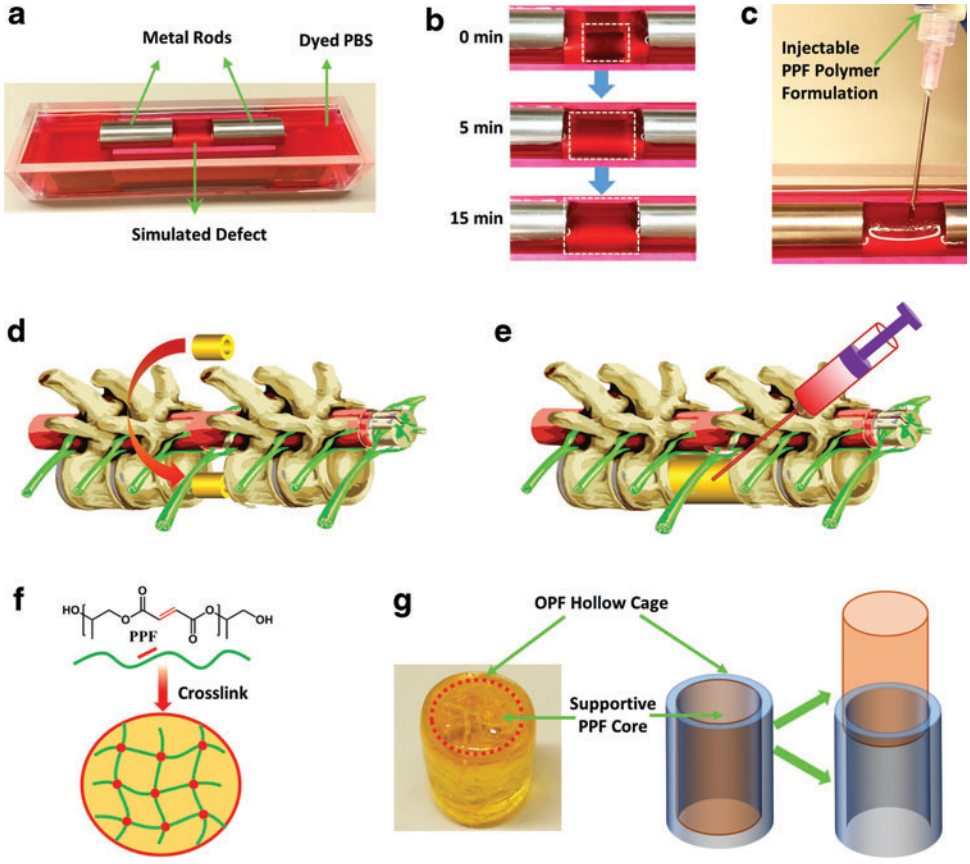

FIG. 7. *In-situ* swelling and injection. **(a)** Molds consisting of metal rods and liquid container were used to mimic the vertebral body defects; **(b)** swelling process of OPF2k cages with 10 mm diameter in PBS at 37°C; **(c)** *in-situ* injection of chemically crosslinkable PPF/BPO/NVP/DMT formulations; **(d)** schematic of the posterior-only surgical insertion of OPF cages; **(e)** *in-situ* swelling and injection of augmentation material PPF for rigidity and support; **(f)** After PPF injection into the scaffold lumen, polymer chains crosslink with each other forming stable networks; **(g)** OPF/PPF composite scaffold, composed of an OPF outlayer containment cage and a stiff supportive PPF core, after *in situ* swelling, injection, and crosslinking. BPO, benzoyl peroxide; DMT, N,N-dimethyl-o-toluidine; NVP, 1-vinyl-2-pyrrolidinone. Color images available online at www.liebertpub.com/tea

the polymer/crosslinker/initiator formulation quickly started the polymerization process forming a stiff scaffold system (Fig. 7f). The OPF scaffold serves as a containment system to allow for *in situ* crosslinking avoiding spreading of the material and minimizing potential side effects and damage to the near tissues. The OPF/PPF composite scaffold, composed of an OPF containment cage outlayer and a solid and stiff supportive PPF core, is shown in Figure 7g.

Discussion

Approximately 1.6 million new cancer cases will be diagnosed during 2016 in the United States[39] and about 50–85% of these patients will develop secondary bone metastases,[40,41] most commonly to the spine.[42] The spine is a load-bearing structure and the presence of vertebral insufficiencies and vertebral body collapse due to metastatic disease significantly decreases the patient's quality of life.[43,44] Survival 1 year after vertebral metastasis is 83.3% in prostate cancer, 77.7% in breast cancer, 51.2% in renal cell carcinoma, and 21.7% in lung cancer.[45] This trend, in some cancer types, for longer survival times than those seen over the past decades, and with an existing demographic shift toward an elderly population, places increased importance on developing treatment strategies that minimize the likelihood of spinal cord injury from either metastatic spinal cord compression or pathologic vertebral fractures.

The choice of treatment for spinal metastases depends on the location and histologic identity of the tumor, the type of reconstruction required, patient comorbidities, their ability to tolerate the required surgical procedure, and the overall extent of their disease. A contained lesion is a ''hole in a bone'' that has intact external margins. A noncontained lesion has missing bone within the normal geometric boundaries of the diseased bone, and, in addition, is missing some or all of those normal geometric bone boundaries. There is currently no injectable biomaterial treatment option available for noncontained metastatic spine defects that can be delivered via less invasive surgical techniques. Current surgical approaches for affected thoracolumbar vertebrae include anterior and posterior approaches such as transperitoneal, retroperitoneal, thoracoabdominal, thoracotomy, sternotomy, posterolateral extracavitary, and posterior transpedicular. These open surgical procedures become difficult to bear by these frail patients. Although the metastatic defect may be replaced with fixed metal or polymeric cages, these implants sometimes require both an anterior and a posterior surgical exposure. While being able to sustain physiologic spine loads, fixed metal implants are not ideal for bone healing in those patients for whom a biologic reconstruction is desired.

Although fixed metal cages have been traditionally used for reconstruction after corpectomy, expandable metal cages have recently gained popularity in the reconstruction of the anterior spinal column following posterior stabilization. Studies have shown the feasibility of using these and fixed cages in the spine without the spread of infection.[46,47] However, little is known about their long-term effect in the spine. A retrospective study by Lau *et al.*[48] showed patients with expandable metal cages to have a significantly higher rate of subsidence, almost double, compared to those with fixed cages at the 1-month visit, and although not significant, this higher rate remained at the 1-year follow-up. Complications have also been reported from such invasive anteroposterior procedures. Schnake *et al.*[49] reported the development of post-thoracotomy syndrome in their patient population. About one-third of their patients presented with complications related to the anterior surgical approach even 5 years postsurgery.

A main disadvantage of fixed cages is migration of the implant, leading to instability of the spine. To prevent migration of the expandable cages, these are often overexpanded intraoperatively. However, this process induces overdistraction of the cages leading to high forces at the adjacent endplates. To reduce the rate of subsidence, Le *et al.*[50] suggested the use of wide intervertebral cages, covering a larger surface area. However, most often it is not feasible to insert these large cages when performing posterolateral or posterior-only approaches, thus leading to much smaller implants or expandable cages. Our proposed biomaterial system would overcome these shortcomings by allowing the insertion of the OPF hollow scaffold from a posterior-only surgical intervention and reducing the surgical burden on these patients. Hydration and expansion to a predetermined larger size would allow for augmentation materials to fill the hollow scaffold to provide stability and support to the spine.

In this *in vitro* experimental study, the swelling time of the OPF scaffolds was determined to be about 20 min. Although scaffolds were hydrated *in vitro* in a PBS-based solution, *in vivo* conditions will present other body fluids, for example, blood, to provide a partial aqueous environment for hydrogel cage swelling. Moreover, the addition of physiological saline solution could be a potential strategy for helping the swelling of hydrogel cages *in situ*. The OPF hydrogel is proven to be biocompatible for both bone and nerve cells in various tissue engineering applications.[51,52] Thus, the OPF applied as a shell material in the OPF/PPF composite material is expected to not present any cytotoxicity and be in an optimum environment for bone tissue regeneration and functional recovery. PPF and its copolymers, on the contrary, are biocompatible, stiff, and mainly serve as bone scaffold materials with excellent support for bone regeneration.[28,29,53,54]

Hydrated OPF is relative bendable and malleable, but the OPF/PPF composite scaffold, due to the mechanical properties of PFF, results in a much rigid structure. According to previous studies, vertebral cancellous bone has been shown to have a compressive modulus in the range of 344 ± 148 MPa.[55] Based on previous work from our group, the PPF material to be implemented as a core in the expandable cage, was reported to have a compressive modulus of 142 ± 7.4 MPa.[18] This is comparable to the lower range of experimentally tested cancellous bone. However, PPF could potentially be modified to include hydroxyapatite to increase its mechanical properties.

This study investigated the effects of various parameters on the swelling time and swelling degree of hydrogel cages, including polymer molecular weight, incorporated charges, and cage diameters. Higher polymer molecular weight, that is, longer polymer chain, resulted in a larger absolute diameter and length cage after hydration. Also, physical incorporation of SMA into the OPF hydrogel network, instead of covalent crosslinking of the molecules, resulted in a shorter expansion time. Final cage size after hydration was also shown to be dependent on the initial cage diameter. These data demonstrate that the ultimate dimension of hydrogel cages can be tailored and well tuned through modulation and optimization of various parameters. This unique property is critical for fulfilling the diverse requirements in

patients of different ages and presenting vertebral insufficiencies in different sections of the spine. Future studies should investigate spinal rigidity and stability *in vitro* with an eventual evaluation of the feasibility of the scaffolds *in vivo.*

Conclusion

The OPF polymeric hydrogel containment device plays a key role in implant function. It has a low cost of preparation and has the ability to be delivered via a less invasive posterior-only surgical procedure compared to the combined anterior and posterior approaches. In addition, on rehydration and expansion to a predetermined size, it allows for injection of augmentation materials through the scaffold wall providing structural support and stability to the spine. OPF cages of varied sizes can be manufactured to meet the specific needs of the patients. *In situ* injection of supportive PPF offers a low-cost OPF/PPF composite system as an alternative to the currently commercialized metal cages.

Acknowledgments

This work was supported by the Mayo Foundation, NIH grants R01-AR56212 and R01-EB03060, and an award from the National Institute of Arthritis and Musculoskeletal and Skin Diseases (Musculoskeletal Research Training Program; T32-AR56950).

Disclosure Statement

No competing financial interests exist.

References

1. Acosta, F.L., Jr., Buckley, J.M., Xu, Z., Lotz, J.C., and Ames, C.P. Biomechanical comparison of three fixation techniques for unstable thoracolumbar burst fractures. Laboratory investigation. J Neurosurg Spine **8,** 341, 2008.
2. Klimo, P., Jr., and Schmidt, M.H. Surgical management of spinal metastases. Oncologist **9,** 188, 2004.
3. Delank, K.S., Wendtner, C., Eich, H.T., and Eysel, P. The treatment of spinal metastases. Dtsch Arztebl Int **108,** 71, 2011.
4. Laufer, I., Sciubba, D.M., Madera, M., Bydon, A., Witham, T.J., Gokaslan, Z.L., and Wolinsky, J.P. Surgical management of metastatic spinal tumors. Cancer Control **19,** 122, 2012.
5. Nathan, S.S., Healey, J.H., Mellano, D., Hoang, B., Lewis, I., Morris, C.D., Athanasian, E.A., and Boland, P.J. Survival in patients operated on for pathologic fracture: implications for end-of-life orthopedic care. J Clin Oncol **23,** 6072, 2005.
6. Cardenas, R.J., Javalkar, V., Patil, S., Gonzalez-Cruz, J., Ogden, A., Mukherjee, D., and Nanda, A. Comparison of allograft bone and titanium cages for vertebral body replacement in the thoracolumbar spine: a biomechanical study. Neurosurgery **66,** 314, 2010.
7. Thongtrangan, I., Balabhadra, R.S., Le, H., Park, J., and Kim, D.H. Vertebral body replacement with an expandable cage for reconstruction after spinal tumor resection. Neurosurg Focus **15,** E8, 2003.
8. Wittenberg, R.H., Moeller, J., Shea, M., White, A.A., 3rd, and Hayes, W.C. Compressive strength of autologous and allogenous bone grafts for thoracolumbar and cervical spine fusion. Spine (Phila Pa 1976) **15,** 1073, 1990.
9. An, H.S., Lynch, K., and Toth, J. Prospective comparison of autograft vs. allograft for adult posterolateral lumbar spine fusion—differences among freeze-dried, frozen, and mixed grafts. J Spinal Disord **8,** 131, 1995.
10. Jeyamohan, S., Vaccaro, A., and Harrop, J. Use of expandable cages in metastasis to the spine. JHN J **4,** 5, 2009.
11. Perrin, R.G., and McBroom, R.J. Anterior versus posterior decompression for symptomatic spinal metastasis. Can J Neurol Sci **14,** 75, 1987.
12. Aebi, M. Spinal metastasis in the elderly. Eur Spine J **12 Suppl 2,** S202, 2003.
13. Armentano, I., Dottori, M., Fortunati, E., Mattioli, S., and Kenny, J.M. Biodegradable polymer matrix nanocomposites for tissue engineering: a review. Polym Degrad Stab **95,** 2126, 2010.
14. Cai, L., Foster, C.J., Liu, X., and Wang, S. Enhanced bone cell functions on poly(epsilon-caprolactone) triacrylate networks grafted with polyhedral oligomeric silsesquioxane nanocages. Polymer **55,** 3836, 2014.
15. Henry, M.G., Cai, L., Liu, X., Zhang, L., Dong, J., Chen, L., Wang, Z., and Wang, S. Roles of hydroxyapatite allocation and microgroove dimension in promoting preosteoblastic cell functions on photocured polymer nanocomposites through nuclear distribution and alignment. Langmuir **31,** 2851, 2015.
16. Thibault, R.A., Baggett, L.S., Mikos, A.G., and Kasper, F.K. Osteogenic differentiation of mesenchymal stem cells on pregenerated extracellular matrix scaffolds in the absence of osteogenic cell culture supplements. Tissue Eng Part A **16,** 431, 2010.
17. Wang, S.F., Lu, L.C., and Yaszemski, M.J. Bone-tissue-engineering material poly(propylene fumarate): correlation between molecular weight, chain dimensions, and physical properties. Biomacromolecules **7,** 1976, 2006.
18. Yan, J., Li, J., Runge, M.B., Dadsetan, M., Chen, Q., Lu, L., and Yaszemski, M.J. Cross-linking characteristics and mechanical properties of an injectable biomaterial composed of polypropylene fumarate and polycaprolactone copolymer. J Biomater Sci Polym Ed **22,** 489, 2011.
19. Nicolas, J., Mura, S., Brambilla, D., Mackiewicz, N., and Couvreur, P. Design, functionalization strategies and biomedical applications of targeted biodegradable/biocompatible polymer-based nanocarriers for drug delivery. Chem Soc Rev **42,** 1147, 2013.
20. Jo, S., Shin, H., Shung, A.K., Fisher, J.P., and Mikos, A.G. Synthesis and characterization of oligo(poly(ethylene glycol) fumarate) macromer. Macromolecules **34,** 2839, 2001.
21. Dhandayuthapani, B., Yoshida, Y., Maekawa, T., and Kumar, D.S. Polymeric scaffolds in tissue engineering application: a review. Int J Polym Sci **2011,** 1687, 2011.
22. Ifkovits, J.L., and Burdick, J.A. Review: photopolymerizable and degradable biomaterials for tissue engineering applications. Tissue Eng **13,** 2369, 2007.
23. Fisher, J.P., Holland, T.A., Dean, D., Engel, P.S., and Mikos, A.G. Synthesis and properties of photocross-linked poly(propylene fumarate) scaffolds. J Biomater Sci Polym Ed **12,** 673, 2001.
24. He, S., Timmer, M.D., Yaszemski, M.J., Yasko, A.W., Engel, P.S., and Mikos, A.G. Synthesis of biodegradable poly(propylene fumarate) networks with poly(propylene fumarate)-diacrylate macromers as crosslinking agents and characterization of their degradation products. Polymer **42,** 1251, 2001.
25. Liu, X., Chen, W., Gustafson, C.T., Miller, A.L., II, Waletzki, B.E., Yaszemski, M.J., and Lu, L. Tunable tissue scaffolds fabricated by in situ crosslink in phase separation system. RSC Adv **5,** 100824, 2015.
26. Liu, X., Miller, A.L., Waletzki, B.E., Yaszemski, M.J., and Lu, L. Novel biodegradable poly(propylene fumarate)-co-

poly(L-lactic acid) porous scaffolds fabricated by phase separation for tissue engineering applications. RSC Adv **5,** 21301, 2015.
27. Cai, L., and Wang, S. Parabolic dependence of material properties and cell behavior on the composition of polymer networks via simultaneously controlling crosslinking density and crystallinity. Biomaterials **31,** 7423, 2010.
28. Kempen, D.H.R., Kruyt, M.C., Lu, L., Wilson, C.E., Florschutz, A.V., Creemers, L.B., Yaszemski, M.J., and Dhert, W.J.A. Effect of autologous bone marrow stromal cell seeding and bone morphogenetic protein-2 delivery on ectopic bone formation in a microsphere/poly(propylene fumarate) composite. Tissue Eng Part A **15,** 587, 2009.
29. Kempen, D.H.R., Lu, L., Hefferan, T.E., Creemers, L.B., Heijink, A., Maran, A., Dhert, W.J.A., and Yaszemski, M.J. Enhanced bone morphogenetic protein-2-induced ectopic and orthotopic bone formation by intermittent parathyroid hormone (1–34) administration. Tissue Eng Part A **16,** 3769, 2010.
30. Kim, C.W., Talac, R., Lu, L., Moore, M.J., Currier, B.L., and Yaszemski, M.J. Characterization of porous injectable poly-(propylene fumarate)-based bone graft substitute. J Biomed Mater ResPart A **85A,** 1114, 2008.
31. Bryant, S.J., and Anseth, K.S. The effects of scaffold thickness on tissue engineered cartilage in photocrosslinked poly(ethylene oxide) hydrogels. Biomaterials **22,** 619, 2001.
32. Kinard, L.A., Kasper, F.K., and Mikos, A.G. Synthesis of oligo(poly(ethylene glycol) fumarate). Nat Protoc **7,** 1219, 2012.
33. Dadsetan, M., Szatkowski, J.P., Yaszemski, M.J., and Lu, L. Characterization of photo-cross-linked oligo poly(ethylene glycol) fumarate hydrogels for cartilage tissue engineering. Biomacromolecules **8,** 1702, 2007.
34. Shin, H., Ruhe, P.Q., Mikos, A.G., and Jansen, J.A. In vivo bone and soft tissue response to injectable, biodegradable oligo(poly(ethylene glycol) fumarate) hydrogels. Biomaterials **24,** 3201, 2003.
35. Temenoff, J.S., Athanasiou, K.A., LeBaron, R.G., and Mikos, A.G. Effect of poly(ethylene glycol) molecular weight on tensile and swelling properties of oligo(poly(ethylene glycol) fumarate) hydrogels for cartilage tissue engineering. J Biomed Mater Res **59,** 429, 2002.
36. Dadsetan, M., Knight, A.M., Lu, L., Windebank, A.J., and Yaszemski, M.J. Stimulation of neurite outgrowth using positively charged hydrogels. Biomaterials **30,** 3874, 2009.
37. Dadsetan, M., Taylor, K.E., Yong, C., Bajzer, Z., Lu, L., and Yaszemski, M.J. Controlled release of doxorubicin from pH-responsive microgels. Acta Biomater **9,** 5438, 2013.
38. Wang, S., Lu, L., Gruetzmacher, J.A., Currier, B.L., and Yaszemski, M.J. Synthesis and characterizations of biodegradable and crosslinkable poly(epsilon-caprolactone fumarate), poly(ethylene glycol fumarate), and their amphiphilic copolymer. Biomaterials **27,** 832, 2006.
39. American Cancer Society. Cancer prevalence: how many people have cancer?. www.cancer.org; 2014.
40. American Academy of Orthopaedic Surgeons. Metastatic bone disease. http://orthoinfo.aaos.org; 2011.
41. Greenlee, R.T., Hill-Harmon, M.B., Murray, T., and Thun, M. Cancer statistics, 2001. CA Cancer J Clin **51,** 15, 2001.
42. Wong, D.A., Fornasier, V.L., and MacNab, I. Spinal metastases: the obvious, the occult, and the impostors. Spine (Phila Pa 1976) **15,** 1, 1990.
43. Ahn, H., Mousavi, P., Roth, S., Reidy, D., Finkelstein, J., and Whyne, C. Stability of the metastatic spine pre and post vertebroplasty. J Spinal Disord Tech **19,** 178, 2006.
44. Latif, T., and Hussein, M.A. Advances in multiple myeloma and spine disease. Clin Lymphoma Myeloma **6,** 228, 2005.
45. Tatsui, H., Onomura, T., Morishita, S., Oketa, M., and Inoue, T. Survival rates of patients with metastatic spinal cancer after scintigraphic detection of abnormal radioactive accumulation. Spine (Phila Pa 1976) **21,** 2143, 1996.
46. Calvert, G., May, L.A., and Theiss, S. Use of Permanently placed metal expandable cages for vertebral body reconstruction in the surgical treatment of spondylodiscities. Orthopedics **37,** e536, 2014.
47. Lu, D.C., Wang, V., and Chou, D. The use of allograft or autograft and expandable titanium cages for the treatment of vertebral osteomyelitis. Neurosurgery **64,** 122, 2009.
48. Lau, D., Song, Y., Guan, Z., La Marca, F., and Park, P. Radiological outcomes of static vs expandable titanium cages after corpectomy: a retrospective cohort analysis of subsidence. Neurosurgery **72,** 529, 2013.
49. Schnake, K.J., Stavridis, S.I., and Kandziora, F. Five-year clinical and radiological results of combined anteroposterior stabilization of thoracolumbar fractures. J Neurosurg Spine **20,** 497, 2014.
50. Le, T.V., Baaj, A.A., Dakwar, E., Burkett, C.J., Murray, G., Smith, D.A., and Uribe, J.S. Subsidence of polyetheretherketone intervertebral cages in minimally invasive lateral retroperitoneal transpsoas lumbar interbody fusion. Spine (Phila Pa 1976) **37,** 1268, 2012.
51. Dadsetan, M., Giuliani, M., Wanivenhaus, F., Brett Runge, M., Charlesworth, J.E., and Yaszemski, M.J. Incorporation of phosphate group modulates bone cell attachment and differentiation on oligo(polyethylene glycol) fumarate hydrogel. Acta Biomater **8,** 1430, 2012.
52. Liu, X., Miller, A.L., II, Park, S., Waletzki, B.E., Terzic, A., Yaszemski, M.J., and Lu, L. Covalent crosslinking of graphene oxide and carbon nanotube into hydrogels enhances nerve cell responses. J Mater Chem B **4**, 6930, 2016.
53. Fang, Z., Giambini, H., Zeng, H., Camp, J.J., Dadsetan, M., Robb, R.A., An, K.N., Yaszemski, M.J., and Lu, L. Biomechanical evaluation of an injectable and biodegradable copolymer P(PF-co-CL) in a cadaveric vertebral body defect model. Tissue Eng Part A **20,** 1096, 2014.
54. Guo, J., Liu, X., Miller, A.L., 2nd, Waletzki, B.E., Yaszemski, M.J., and Lu, L. Novel porous poly(propylene Fumarate-co-caprolactone) scaffolds fabricated by thermally induced phase separation. J Biomed Mater Res A 2016 [Epub ahead of print]; DOI: 10.1002/jbm.a.35862.
55. Morgan, E.F., and Keaveny, T.M. Dependence of yield strain of human trabecular bone on anatomic site. J Biomech **34,** 569, 2001.

Address correspondence to:
Lichun Lu, PhD
Department of Physiology and Biomedical Engineering
Mayo Clinic
200 First Street SW
Rochester, MN 55905

E-mail: lu.lichun@mayo.edu

Received: June 21, 2016
Accepted: November 1, 2016
Online Publication Date: December 26, 2016